Subradiant Emission from Regular Atomic Arrays: Universal Scaling of Decay Rates from the Generalized Bloch Theorem

Yu-Xiang Zhang[1,*] and Klaus Mølmer[2,†]
[1]Niels Bohr Institute, University of Copenhagen, Blegdamsvej 17, 2100 Copenhagen Ø, Denmark
[2]Center for Complex Quantum Systems, Department of Physics and Astronomy, Aarhus University, 8000 Aarhus C, Denmark

(Received 25 June 2020; accepted 13 November 2020; published 14 December 2020)

The Hermitian part of the field-mediated dipole-dipole interaction in infinite periodic arrays of two-level atoms yields an energy band of the singly excited states. In this Letter, we show that a dispersion relation, $\omega_k - \omega_{k_{ex}} \propto (k - k_{ex})^s$, near the band edge of the infinite system leads to the existence of subradiant states of finite one-dimensional arrays of N atoms with decay rates scaling as $N^{-(s+1)}$. This explains the recently discovered N^{-3} scaling and it leads to the prediction of power law scaling with higher power for special values of the lattice period. For the quantum optical implementation of the Su-Schrieffer-Heeger topological model in a dimerized emitter array, the band gap closing inherent to topological transitions changes the value of s in the dispersion relation and alters the decay rates of the subradiant states by many orders of magnitude.

DOI: 10.1103/PhysRevLett.125.253601

Subradiance is the phenomenon that radiative emission by an atomic ensemble is collectively prohibited [1] in contrast to the factor N^2 enhancement of the radiation rate by N emitters in Dicke superradiance [2]. The application of the subradiant suppression of radiative decay in quantum memories [3,4], excitation transfer [5–7], and topological photonics [8,9] has spurred strong interests and a number of results have been obtained that are not yet well understood in a single comprehensive theory. Recently, one-dimensional (1D) emitter arrays with subwavelength separations, see Fig. 1(a), were found to have subradiant states with decay rates scaling as N^{-3} [10–17], but examples of rates scaling with $N^{-\alpha}$ with $\alpha > 3$ were also soon identified [18].

The close relationship between subradiance and the band flatness of collectively shared atomic excitations has been realized to be a crucial component of the collective dipole-dipole interaction [19], see also Refs. [20–31]. In this Letter we show that a better understanding of precisely this relationship can explain and predict several characteristics of subradiance.

Dipole-dipole interaction.—In regimes where the Born-Markov approximation works well, one can trace out the quantized light fields and obtain the field-mediated dipole-dipole couplings between the emitters described by an effective Hamiltonian [32]:

$$H_{\text{eff}} = -\mu_0\omega_0^2 \sum_{m,n=1}^{N} \mathbf{d}_m^* \cdot \mathbf{G}(x_m - x_n, \omega_0) \cdot \mathbf{d}_n \sigma_m^\dagger \sigma_n, \quad (1)$$

where ω_0 is the transition frequency between the emitter ground state $|g\rangle$ and the excited state $|e\rangle$, $\sigma_m = |g_m\rangle\langle e_m|$, $\mathbf{d}_m$ and x_m are the transition dipole moment and spatial coordinate of the mth atom, μ_0 is the vacuum permeability and $\mathbf{G}$ is the dyadic Green's tensor. Our main example is atom arrays along a single dimension in 3D free space, where atoms are equally separated by d and transition dipoles are polarized transversally to the lattice direction as depicted in Fig. 1(a).

Restricting our analysis to the case of a single excitation, shared among the atoms, H_{eff} is formally equivalent to a non-Hermitian tunneling Hamiltonian among the discrete sites m, representing the localized excitation, $|m\rangle = \sigma_m^\dagger|G\rangle$,

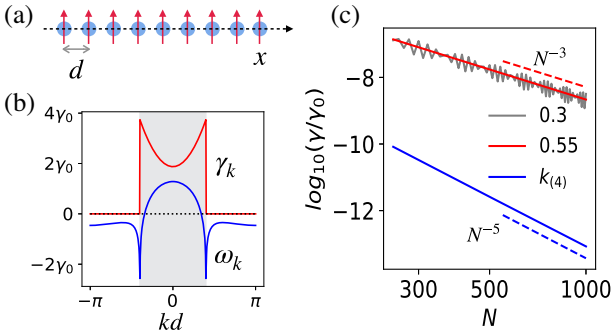

FIG. 1. (a) Illustration of a regular array of emitters with dipole moments aligned perpendicular to the spatial array. (b) Energy shifts ω_k (lower blue curve) and decay rates γ_k (upper red curve) for the emitter array with $k_0 d/\pi = 0.4$, where $k_0 c$ is the atomic resonance frequency. Wave numbers outside the shaded interval $\Gamma = [-k_0, k_0]$ correspond to frequencies exceeding the atomic resonance frequency. (c) Decay rates of the most subradiant states of finite arrays with N emitters in units of the single emitter spontaneous emission rate γ_0, for $k_0 d/\pi = 0.3$ (gray curve), 0.55 (red curve), and 0.4828 (lower blue curve). The dashed lines show N^{-3} and N^{-5} dependencies.

where $|G\rangle = |g_1 g_2 \cdots g_N\rangle$. For an *infinite* array with $-\infty < n, m < \infty$, the dipole-dipole interaction Hamiltonian, $H_{\rm eff}^{\infty}$, has singly excited eigenstates in the form of Bloch states, $|k\rangle = \sum_{m=-\infty}^{\infty} e^{ikx_m}|m\rangle$, with $k \in [-\pi/d, \pi/d]$ and complex eigenvalues $\omega_k - i\gamma_k/2$. In Fig. 1(b), the energy shift ω_k and the decay rate γ_k are shown for these states with $k_0 = 0.4\pi/d$ ($k_0 = \omega_0/c$, c is the speed of light). Notably, γ_k vanishes outside $\Gamma = [-k_0, k_0]$, because the corresponding optical frequencies are not resonant with the atoms [12].

In the following, we shall make use of the fact that $H_{\rm eff} = P_N H_{\rm eff}^{\infty} P_N$, where P_N projects on the space with no excitations outside the sites $1, 2 \cdots N$. This implies that the singly excited eigenstates of $H_{\rm eff}$ can be expanded on the Bloch states, restricted to the N lattice sites and normalized. We shall refer to these states by the complex argument $z = e^{ikd}$,

$$|z = e^{ikd}\rangle = \frac{1}{\sqrt{N}} \sum_{m=1}^{N} e^{ikx_m}|m\rangle, \tag{2}$$

and thus write

$$H_{\rm eff} = N \int_{-\pi/d}^{\pi/d} \frac{dk}{2\pi/d} \left(\omega_k - \frac{i}{2}\gamma_k\right) |e^{ikd}\rangle\langle e^{ikd}|. \tag{3}$$

Note that the states $|e^{ikd}\rangle$ are not orthogonal, and hence not the eigenstates of $H_{\rm eff}$. Therefore, in finite arrays states with $k \notin \Gamma$ are candidate subradiant states with tiny but finite decay rates.

Generalized Bloch theorem.—To identify the singly excited eigenstates of the finite atomic arrays, the generalized Bloch theorem [33–35] is essential. The theorem is established for Hamiltonians in the general form of

$$H_R = h_0 \mathbb{I} + \sum_{r=1}^{R} \sum_{m=1}^{N-r} h_r |m\rangle\langle m+r| + h_r^* |m+r\rangle\langle m|, \tag{4}$$

where h_r are coupling (tunneling) strengths across sites separated by up to a maximum range of R. H_R is periodic in m except for the leftmost sites $\partial_l = \{1, 2, \ldots R\}$ and the, similarly defined, rightmost sites ∂_r. We denote the projection onto the "boundary" $\partial = \partial_l \cup \partial_r$ by P_∂, while the projector on the "bulk" sites is denoted by P_B with $P_\partial + P_B = P_N$.

To find eigenstates fulfilling $H_R|\psi\rangle = E|\psi\rangle$, we apply the generalized Bloch theorem noting that the solution space of the *bulk equation* $P_B(H_R - E)|\psi\rangle = 0$ is spanned by the states $|z = e^{ikd}\rangle$, where z are the roots of the equation $\tilde{\omega}_R(z) = E$ with

$$\tilde{\omega}_R(z) = h_0 + \sum_{r=1}^{R} (h_r z^r + h_r^* z^{-r}). \tag{5}$$

As the array is finite, states $|z\rangle$ with complex k (or, equivalently, $|z| \neq 1$) are also physically permitted. This implies that all the complex roots z_j of the $2R$-degree polynomial equation (5), should be identified. The eigenstate of H_R can then be written as the superposition $|\psi\rangle = \sum_{j=1}^{2R} c_j |z_j\rangle$ that fulfills the boundary conditions, i.e., $P_\partial(H_R - E)|\psi\rangle = 0$.

We note that Eq. (5) yields the dispersion relation of H_R, $\omega_R(k) = \tilde{\omega}_R(e^{ikd})$, and now suppose that $\omega_R(k)$ has an extremum point $k_{\rm ex}$ of degree s, i.e., $\omega_R(k) \approx \omega_R(k_{\rm ex}) + a_s(k - k_{\rm ex})^s$ for $k \approx k_{\rm ex}$, with s an even integer and a_s the Taylor expansion coefficient. Then $\tilde{\omega}_R(z)$ can be expanded around $z_{\rm ex} = e^{ik_{\rm ex}d}$ as

$$\tilde{\omega}_R(z) = \tilde{\omega}_R(z_{\rm ex}) + a_s \frac{1}{(id z_{\rm ex})^s} (z - z_{\rm ex})^s + \cdots. \tag{6}$$

We now focus on eigenstates of the finite system with eigenvalues $E \approx \omega_R(k_{\rm ex})$. Since the system has N singly excited eigenstates, it is reasonable to assume that two neighboring states have wave numbers separated by $O(N^{-1})\pi/d$, and hence a series of eigenvalues may exist with $E = \omega_R(k_{\rm ex}) + (a_s/d^s)\delta^s$, where $\delta \sim N^{-1}$. Equation (6) thus yields s roots of $\tilde{\omega}_R(z) = E$ close to $z_{\rm ex}$:

$$z_j \approx z_{\rm ex}(1 + i\delta e^{i2\pi(j/s)}), \quad j = 1, 2 \cdots s, \tag{7}$$

while the remaining $2R - s$ roots are not in the vicinity of $z_{\rm ex}$.

A simpler Hamiltonian.—For a given H_R, these exists a Hamiltonian, $\mathbf{H}_{s/2}$, which has its extremum energy at the same $k_{\rm ex}$ as H_R and a dispersion relation of the same degree s, $\tilde{\omega}_{s/2}(z) = \tilde{\omega}_{s/2}(z_{\rm ex}) + a_s(-d^2 z_{\rm ex} z)^{-s/2}(z - z_{\rm ex})^s$. $\mathbf{H}_{s/2}$ is chosen such that the roots of $\tilde{\omega}_{s/2}(z) = E$ are given exactly by Eq. (7). We shall show that the eigenstates of $\mathbf{H}_{s/2}$ approximate the singly excited subradiant eigenstates of $H_{\rm eff}$ well and permit evaluation of their decay rates by perturbation theory.

By introducing ϵ_j and η_j so that $z_j/z_{\rm ex} = (1 + \epsilon_j)^{-1} = 1 + \eta_j$, we find that the boundary condition implies [36]

$$\sum_{j=1}^{s} c_j \epsilon_j^r = 0, \qquad \sum_{j=1}^{s} c_j z_j^{N+1} \eta_j^r = 0, \tag{8}$$

for all powers $r = 0, 1, 2, \ldots, s/2 - 1$. Equation (8) and the smallness of $\epsilon_j, \eta_j \sim N^{-1}$ are sufficient to provide effective solutions of the problem without explicitly determining $\{c_j\}$ and $\{\epsilon_j, \eta_j\}$.

Perturbative calculation of the subradiant decay rates.—While $H_{\rm eff}$ represented by $\mathbf{G}(x_m - x_n, \omega_0)$ in Eq. (1) does not have a bounded tunneling range, we shall demonstrate that for values of k near $k_{\rm ex} \notin \Gamma$, $H_{\rm eff} - \mathbf{H}_{s/2}$ can be treated as a perturbation to $\mathbf{H}_{s/2}$. The non-Hermitian $H_{\rm eff}$ can be separated into a coherent part and a dissipative part, $H_{\rm eff} = H_{\rm eff}^{\rm Re} - iH_{\rm eff}^{\rm Im}$, cf., Eq. (3). The decay rates of the

subradiant eigenstates of $H_{\rm eff}$ can therefore be approximated by $\gamma = 2\langle\psi|H_{\rm eff}^{\rm Im}|\psi\rangle$, evaluated in the eigenstates of $\mathbf{H}_{s/2}$.

Following Eq. (3), we must evaluate $\langle e^{ikd}|\psi\rangle$ for $k \in \Gamma = [-k_0, k_0]$:

$$\langle e^{ikd}|\psi\rangle = \frac{1}{N}\sum_{j=1}^{s} c_j \frac{z_j e^{-ikd} - (z_j e^{-ikd})^{N+1}}{1 - z_j e^{-ikd}}. \tag{9}$$

Separating the terms in the enumerator and expanding z_j in terms of ϵ_j and η_j, we obtain two contributions:

$$\sum_{j=1}^{s} c_j \frac{z_j e^{-ikd}}{1 - z_j e^{-ikd}} = \sum_{j=1}^{s} c_j \frac{1}{z_j^{-1} e^{ikd} - 1} = \frac{1}{z_{\rm ex}^{-1} e^{ikd} - 1} \sum_{n=0}^{\infty} \frac{\sum_{j=1}^{s} c_j \epsilon_j^n}{(z_{\rm ex} e^{-ikd} - 1)^n}, \tag{10a}$$

$$\sum_{j=1}^{s} c_j \frac{(z_j e^{-ikd})^{N+1}}{1 - z_j e^{-ikd}} = \frac{e^{-i(N+1)kd}}{1 - z_{\rm ex} e^{-ikd}} \sum_{n=0}^{\infty} \frac{\sum_{j=1}^{s} c_j z_j^{N+1} \eta_j^n}{(e^{ikd} - z_{\rm ex})^n}, \tag{10b}$$

where terms with $n = 0, 1, \ldots, s/2 - 1$ vanish due to Eq. (8).

Keeping only the nonvanishing term of the lowest order, $n = s/2$, we obtain

$$\langle\psi|H_{\rm eff}^{\rm Im}|\psi\rangle \le \frac{1}{N}\left(|\sum_j c_j \epsilon_j^{s/2}|^2 + |\sum_j c_j z_j^{N+1} \eta_j^{s/2}|^2\right) \times \int_{-k_0}^{k_0} \frac{dk}{2\pi/d} \frac{\gamma_k}{|z_{\rm ex} - e^{ikd}|^{s+2}}. \tag{11}$$

As $k_{\rm ex} \notin \Gamma$, the denominator in the integral does not approach 0, and the integral contributes an N-independent finite factor. Using $\epsilon_j \sim \eta_j \sim N^{-1}$, we thus get the scaling of the decay rate with N,

$$\gamma = 2\langle\psi|H_{\rm eff}^{\rm Im}|\psi\rangle \sim N^{-s-1}. \tag{12}$$

This yields the advertised $N^{-\alpha}$ power law with $\alpha = s + 1$. Note that $\langle\psi|H_{\rm eff}^{\rm Im}|\psi\rangle$ is a factor N^{-1} smaller than the differences between the real eigenvalues of $\mathbf{H}_{s/2}$ in the vicinity of $\omega_R(k_{\rm ex})$. Thus the perturbation treatment is consistent in the limit of large N.

To complete the demonstration, we must also ensure that $\Delta H = H_{\rm eff}^{\rm Re} - \mathbf{H}_{s/2}$ can be consistently treated as a perturbation. To this end, we represent ΔH in the form of Eq. (3), with the dispersion relation $\delta\omega_k = \omega_k - \omega_{s/2}(k)$ and exploit the fact that $\delta\omega_k \sim N^{-s-1}$ for $k \approx k_{\rm ex}$. See more details in the Supplemental Material [36].

As a further check of the consistency of our perturbative treatment, we verify that the numerical right eigenstates of $H_{\rm eff}$, differ by only a small amount from the eigenstates of the simpler Hamiltonian

$$|\psi'\rangle \propto |\psi\rangle + O(N^{-1})|\psi^{\perp}\rangle \tag{13}$$

yielding an infidelity of, $1 - |\langle\psi|\psi'\rangle|^2 \sim N^{-2}$.

The N^{-2} scaling of the infidelity is, indeed, confirmed for the subradiant states of our system with decay rates scaling as N^{-3} for $k_0 d/\pi = 0.3$ and 0.55 (gray and red curves in Fig. 2), and for the subradiant state with a decay rate scaling as N^{-5} and $k_0 d/\pi = k_{(4)} \approx 0.4828$ (blue curve). We observe that the gray infidelity curve for $k_0 = 0.3\pi/d$ follows the overall N^{-2} behavior with dramatic oscillations, which are due to an interference effect [19] between Bloch waves that are degenerate with the extremum of ω_k. This interference is also the cause of the oscillatory structures in the value of the decay rate as function of N in Fig. 1(d). The upper panel of Fig. 2 shows the 2nd and 4th order coefficients ($a_{2,4}$) of the Taylor series of ω_k at $k_{\rm ex} = \pi/d$, and we see that $a_2 > 0$ and $a_4 < 0$ when $k_0 < k_{(4)}$ and hence band degeneracy is expected, as illustrated in the inset of Fig. 2. For $k_0 \ge k_{(4)}$, the extremum is nondegenerate and no oscillations are observed. A similar behavior is displayed in Ref. [36] for analytically solvable toy model Hamiltonians.

Qualitative discussion of subradiant decay rates.—A supplementary, qualitative explanation of why a higher order dispersion relation leads to a higher order $N^{-\alpha}$ decay rate may be inferred from Fig. 3(b) in Ref. [12], which

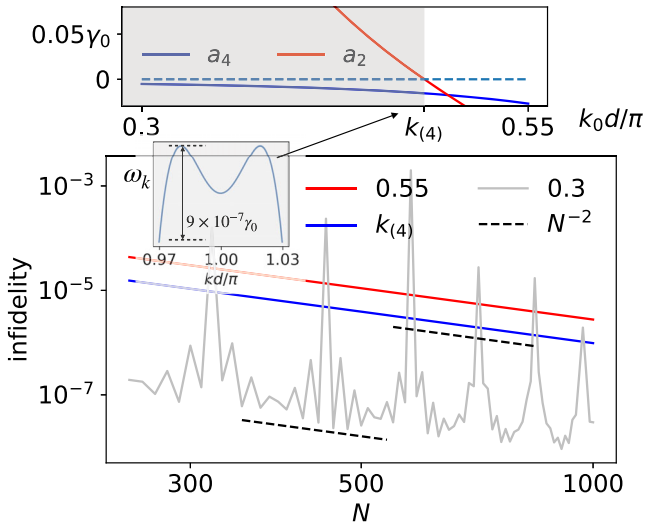

FIG. 2. Upper panel: coefficients of the 2nd and 4th order terms of the Taylor series ($a_{2,4}$) of the dispersion relation around $k = \pi/d$, as a function of $k_0 d/\pi$. Lower panel: infidelities (log scale) between the most subradiant right eigenstates of $H_{\rm eff}$ for $k_0 d/\pi = 0.3$, 0.55 and $k_0 = k_{(4)}$, and the eigenstates of $\mathbf{H}_1$ and $\mathbf{H}_2$, respectively. The dashed lines indicate the N^{-2} power law behavior. Inset: the dependence of ω_k on k near $k_{\rm ex} = \pi/d$, for $k_0 = 0.4826\pi/d < k_{(4)}$.

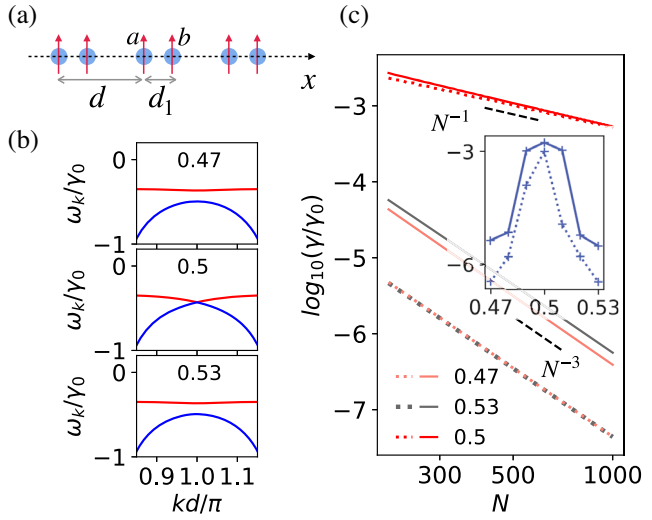

FIG. 3. (a) The dimerized array of atomic emitters. (b) Dispersion relations for the dimerized array with $k_0 = 0.8\pi/d$ and $d_1/d = 0.47$, 0.5, 0.53, respectively. (c) Decay rates of the subradiant states with wave numbers close to π/d as a function of the number of units cells N. The dashed lines show the reference N^{-1} and N^{-3} power law dependence for comparison with the numerical results. The inset shows the decay rate as function of d_1/d for $N = 500$. The dotted (solid) lines refer to the upper (lower) band.

shows that the radiation from the subradiant states is mostly emitted from the ends of the emitter array. A flat band structure with a larger value of s implies a slower group velocity which extends the excitation lifetime in the system by impeding the propagation of excitation towards the chain ends.

By the same argument, we expect that subradiant states well inside the energy bands, i.e., in regions of linear dispersion, are characterized by finite group velocities and hence the emission from the ends of the array occur with a rate scaling as N^{-1}. In conjunction with their numerical discovery of subradiant states with $\sim N^{-3}$ decay rates, Asenjo-Garcia *et al.* [12] identified a series of states labeled by an integer ξ and decaying at rates $\sim \xi^2/N^3$. For $\xi \sim O(N)$, corresponding to wave numbers well inside the energy bands ($k - k_{ex} \simeq \xi\pi/Nd$ [14]), this, indeed, yields decay rates scaling as N^{-1}.

Our results imply that varying the power s of the energy band may form practical ways to control the emission of light by emitter arrays. In the remaining part of this Letter, we shall demonstrate such control in emitter arrays that undergo a Su-Schrieffer-Heeger (SSH) type topological transition.

Dimerized arrays implementing the SSH Hamiltonian.— We proceed with the study of a dimerized atomic array interacting with the quantized electromagnetic field in 3D free space and in a 1D waveguide. Both systems have topological properties characterized by the SSH model [37]. For a recent review on topological Bloch bands, see Ref. [38]. Topological transitions are usually accompanied by the closing and opening of gaps in the energy bands. The above analysis suggests that this may radically impact the radiative decay rates of the subradiant states.

Figure 3(a) shows the dimerized version of the emitter array, which has the lattice constant d and two atoms (denoted by "a, b") separated by the distance d_1 within each unit cell. We denote $d_2 = d - d_1$. Two nonequivalent configurations, $d_1 < d_2$ and $d_1 > d_2$, are found to be topologically trivial and nontrivial (manifested by boundary states [39,40]) and the band topology can be characterized mathematically by the Zak phase [41]. The topological phase transition occurs at $d_1 = d_2$, where we recover the regular array in Fig. 1(a) with the lattice constant d_1. The subradiant states with, e.g., $k = \pm 0.5\pi/d_1$ (and $k_0 = 0.4\pi/d_1$) are well within the regions with linear dispersion, and they have decay rates scaling as N^{-1}. The lowest band of the Brillouin zone of the regular lattice $[-\pi/d_1, \pi/d_1]$ corresponds to two bands of the Brillouin zone of the dimerized lattice $[-\pi/d, \pi/d]$, where the subradiant states are labeled by $k = \pi/d$ (and where $k_0 = 0.8\pi/d$). To describe the two Bloch bands, Eq. (2) should be augmented with intracell states

$$|e^{ikd}, \mathbf{u}^{\pm}\rangle = \frac{1}{\sqrt{N}} \sum_{m=1}^{N} e^{ikx_m} \mathbf{u}^{\pm} \cdot \boldsymbol{\sigma}_m^{\dagger} |G\rangle, \tag{14}$$

where $\boldsymbol{\sigma}_m^{\dagger} = (\sigma_{m,a}^{\dagger}, \sigma_{m,b}^{\dagger})$, the unit vector $\mathbf{u}^{\pm} = (u_a^{\pm}, u_b^{\pm})$ describes the relative excitation amplitudes inside each unit cell, and "$+(-)$" labels the upper(lower) band. As illustrated in the middle panel of Fig. 3(b), the two bands of real eigenenergies cross at $k = \pi/d$ with linear dispersion relations.

However, whenever $d_1 \neq d_2$, a band gap opens at $k = \pi/d$. This is illustrated in the top and bottom panels of Fig. 3(b) for $d_1/d = 0.47$ and 0.53, respectively. When the gap forms, both the upper and lower bands show a quadratic dispersion ($s = 2$) around $k = \pi/d$, and we expect the radiative behavior to change significantly. This, indeed, occurs as evidenced in Fig. 3(c) where we plot the dependence of the decay rate on N for the subradiant states with wave number close to $k_{\mathrm{ex}} = \pi/d$ for both bands and for the three values of d_1/d. Our numerical calculations clearly show how the N^{-1} dependence of the decay rate for $d_1 = d/2$ changes to N^{-3} in case of $d_1/d = 0.47$ and 0.53. An enlargement of the transition is shown in the inset of Fig. 3(c) for the array emitting into the 3D quantized field with $k_0 = 0.8\pi/d$ and $N = 500$. Notably, the decay rates decrease by 3 orders of magnitude away from the topological transition. Such critical phenomenon may thus be used to witness aspects of the topological transition.

Analytical results can be obtained for the dimerized arrays coupled to an ideal 1D waveguide. The effective Hamiltonian [42]

$$H_{1D} = -i\frac{\gamma_0}{2}\sum_{\substack{m,n=1\\ \mu,\nu\in\{a,b\}}}^{N} e^{ik_0|x_{m,\mu}-x_{n,\nu}|}\sigma^{\dagger}_{m,\mu}\sigma_{n,\nu} \tag{15}$$

has an inverse, H_{1D}^{-1} that is almost identical to the original SSH model [19,36]. Hence H_{1D} supports the SSH type topology and the critical points are found to be $d_1 = d_2$ and $d_1 = d_2 \pm \pi/k_0$. In Ref. [36] we focus on the latter values causing the band gap opening and closing to occur around $k = 0$. At the precise value, $d_1 = d_2 \pm \pi/k_0$, the subradiant states with wave numbers close to $k = 0$ have decay rates given by [36]

$$\gamma = \frac{\gamma_0}{4N}\cot(k_0 d_1)\ln\left(\frac{1+\sin k_0 d_1}{1-\sin k_0 d_1}\right). \tag{16}$$

The N^{-1} scaling of the subradiant decay rates transitions to N^{-3} when $d_1 \neq d_2 \pm \pi/k_0$.

Conclusions.—We have presented a derivation of a universal connection between the decay rates of the most subradiant states of an array of N two level emitters and the Bloch wave dispersion relation near the band edge. This result was demonstrated and explained in detail and it confirms the intrinsic connection between subradiant states and flat energy bands, emphasized in Ref. [19]. We studied the case of radiative emission into the 3D quantized electromagnetic field and a 1D waveguide, but we note that the subradiant phenomena may be further manipulated by coupling to structured radiation reservoirs, such as photonic flat bands [43]. Also, extension of our theory to arrays in two and three dimensions may provide an interesting research area.

Our study concerned only the linear regime of a single excitation, while we have previously shown that pairs of excitations may survive for even longer times than single excitations in the system [44]. A promising avenue for further research would thus be the exploration of subradiance with many excitations in systems with flat energy bands. Such studies may pose analogies with phenomena in strongly correlated many-body physics, such as, e.g., the fractional Hall effect [45,46] and the Lieb lattice [47,48], see also Refs. [38,49].

Y.-X. Zhang acknowledges financial support from the Danish National Research Foundation and the European Union's Horizon 2020 Research and Innovation Program under Grant Agreement No. 820445 (Quantum Internet Alliance). K. M. acknowledges support from the Danish National Research Foundation through the Center of Excellence CCQ (Grant Agreement No. DNRF156).

*iyxz@nbi.ku.dk
†moelmer@phys.au.dk

[1] P. Weiss, M. O. Araújo, R. Kaiser, and W. Guerin, New J. Phys. **20**, 063024 (2018).
[2] R. H. Dicke, Phys. Rev. **93**, 99 (1954).
[3] G. Facchinetti, S. D. Jenkins, and J. Ruostekoski, Phys. Rev. Lett. **117**, 243601 (2016).
[4] M. T. Manzoni, M. Moreno-Cardoner, A. Asenjo-Garcia, J. V. Porto, A. V. Gorshkov, and D. E. Chang, New J. Phys. **20**, 083048 (2018).
[5] M. Moreno-Cardoner, D. Plankensteiner, L. Ostermann, D. E. Chang, and H. Ritsch, Phys. Rev. A **100**, 023806 (2019).
[6] J. A. Needham, I. Lesanovsky, and B. Olmos, New J. Phys. **21**, 073061 (2019).
[7] K. E. Ballantine and J. Ruostekoski, Phys. Rev. Research **2**, 023086 (2020).
[8] J. Perczel, J. Borregaard, D. E. Chang, H. Pichler, S. F. Yelin, P. Zoller, and M. D. Lukin, Phys. Rev. Lett. **119**, 023603 (2017).
[9] R. J. Bettles, J. c. v. Minář, C. S. Adams, I. Lesanovsky, and B. Olmos, Phys. Rev. A **96**, 041603(R) (2017).
[10] H. R. Haakh, S. Faez, and V. Sandoghdar, Phys. Rev. A **94**, 053840 (2016).
[11] T. S. Tsoi and C. K. Law, Phys. Rev. A **78**, 063832 (2008).
[12] A. Asenjo-Garcia, M. Moreno-Cardoner, A. Albrecht, H. J. Kimble, and D. E. Chang, Phys. Rev. X **7**, 031024 (2017).
[13] A. Albrecht, L. Henriet, A. Asenjo-Garcia, P. B. Dieterle, O. Painter, and D. E. Chang, New J. Phys. **21**, 025003 (2019).
[14] Y.-X. Zhang and K. Mølmer, Phys. Rev. Lett. **122**, 203605 (2019).
[15] T. Yu, Y.-X. Zhang, S. Sharma, X. Zhang, Y. M. Blanter, and G. E. W. Bauer, Phys. Rev. Lett. **124**, 107202 (2020).
[16] F. Dinc, L. E. Hayward, and A. M. Brańczyk, Phys. Rev. Research **2**, 043149 (2020).
[17] J. D. Brehm, A. N. Poddubny, A. Stehli, T. Wolz, H. Rotzinger, and A. V. Ustinov, arXiv:2006.03330.
[18] D. F. Kornovan, N. V. Corzo, J. Laurat, and A. S. Sheremet, Phys. Rev. A **100**, 063832 (2019).
[19] A. N. Poddubny, Phys. Rev. A **101**, 043845 (2020).
[20] A. Asenjo-Garcia, H. J. Kimble, and D. E. Chang, Proc. Natl. Acad. Sci. U.S.A. **116**, 25503 (2019).
[21] S. D. Jenkins, J. Ruostekoski, N. Papasimakis, S. Savo, and N. I. Zheludev, Phys. Rev. Lett. **119**, 053901 (2017).
[22] M. Mirhosseini, E. Kim, X. Zhang, A. Sipahigil, P. B. Dieterle, A. J. Keller, A. Asenjo-Garcia, D. E. Chang, and O. Painter, Nature (London) **569**, 692 (2019).
[23] P.-O. Guimond, A. Grankin, D. V. Vasilyev, B. Vermersch, and P. Zoller, Phys. Rev. Lett. **122**, 093601 (2019).
[24] E. Shahmoon, D. S. Wild, M. D. Lukin, and S. F. Yelin, Phys. Rev. Lett. **118**, 113601 (2017).
[25] J. Rui, D. Wei, A. Rubio-Abadal, S. Hollerith, J. Zeiher, D. M. Stamper-Kurn, C. Gross, and I. Bloch, Nature (London) **583**, 369 (2020).
[26] R. Bekenstein, I. Pikovski, H. Pichler, E. Shahmoon, S. F. Yelin, and M. D. Lukin, Nat. Phys. **16**, 676 (2020).
[27] Y.-X. Zhang, Y. Zhang, and K. Mølmer, Phys. Rev. A **98**, 033821 (2018).
[28] Y. Ke, A. V. Poshakinskiy, C. Lee, Y. S. Kivshar, and A. N. Poddubny, Phys. Rev. Lett. **123**, 253601 (2019).
[29] N. J. Schilder, C. Sauvan, Y. R. P. Sortais, A. Browaeys, and J.-J. Greffet, Phys. Rev. Lett. **124**, 073403 (2020).
[30] R. J. Bettles, M. D. Lee, S. A. Gardiner, and J. Ruostekoski, Commun. Phys. **3**, 141 (2020).

[31] J. Cremer, D. Plankensteiner, M. Moreno-Cardoner, L. Ostermann, and H. Ritsch, arXiv:2004.09861.
[32] H. T. Dung, L. Knöll, and D.-G. Welsch, Phys. Rev. A **66**, 063810 (2002).
[33] A. Alase, E. Cobanera, G. Ortiz, and L. Viola, Phys. Rev. Lett. **117**, 076804 (2016).
[34] E. Cobanera, A. Alase, G. Ortiz, and L. Viola, J. Phys. A **50**, 195204 (2017).
[35] A. Alase, E. Cobanera, G. Ortiz, and L. Viola, Phys. Rev. B **96**, 195133 (2017).
[36] See Supplemental Material at http://link.aps.org/supplemental/10.1103/PhysRevLett.125.253601 for detailed derivations and analytical results.
[37] W. P. Su, J. R. Schrieffer, and A. J. Heeger, Phys. Rev. Lett. **42**, 1698 (1979).
[38] N. R. Cooper, J. Dalibard, and I. B. Spielman, Rev. Mod. Phys. **91**, 015005 (2019).
[39] B. X. Wang and C. Y. Zhao, Phys. Rev. A **98**, 023808 (2018).
[40] S. R. Pocock, X. Xiao, P. A. Huidobro, and V. Giannini, ACS Photonics **5**, 2271 (2018).
[41] M. Atala, M. Aidelsburger, J. T. Barreiro, D. Abanin, T. Kitagawa, E. Demler, and I. Bloch, Nat. Phys. **9**, 795 (2013).
[42] D. E. Chang, L. Jiang, A. V. Gorshkov, and H. J. Kimble, New J. Phys. **14**, 063003 (2012).
[43] D. Leykam and S. Flach, APL Photonics **3**, 070901 (2018).
[44] Y.-X. Zhang, C. Yu, and K. Mølmer, Phys. Rev. Research **2**, 013173 (2020).
[45] J. Perczel, J. Borregaard, D. E. Chang, S. F. Yelin, and M. D. Lukin, Phys. Rev. Lett. **124**, 083603 (2020).
[46] S. A. Parameswaran, R. Roy, and S. L. Sondhi, C.R. Phys. **14**, 816 (2013).
[47] S. Mukherjee, A. Spracklen, D. Choudhury, N. Goldman, P. Öhberg, E. Andersson, and R. R. Thomson, Phys. Rev. Lett. **114**, 245504 (2015).
[48] N. Goldman, D. F. Urban, and D. Bercioux, Phys. Rev. A **83**, 063601 (2011).
[49] D. Leykam, A. Andreanov, and S. Flach, Adv. Phys. X **3**, 1473052 (2018).